View metadata, citation and similar papers at core.ac.uk

brought to you by CORE

provided by Aston Publications Explorer

Loughborough University

This item was submitted to Loughborough's Institutional Repository by the author and is made available under the following Creative Commons Licence conditions.

creative commons

COMMONS DEED

Attribution-NonCommercial-NoDerivs 2.5

You are free:

- to copy, distribute, display, and perform the work

Under the following conditions:

Attribution. You must attribute the work in the manner specified by the author or licensor.

Noncommercial. You may not use this work for commercial purposes.

No Derivative Works. You may not alter, transform, or build upon this work.

- For any reuse or distribution, you must make clear to others the license terms of this work.
- Any of these conditions can be waived if you get permission from the copyright holder.

Your fair use and other rights are in no way affected by the above.

This is a human-readable summary of the Legal Code (the full license).

Disclaimer

For the full text of this licence, please go to:
http://creativecommons.org/licenses/by-nc-nd/2.5/

revised

11th November 2006

Layer-by-Layer Deposition of Open-Pore Mesoporous TiO_2 – Nafion® Film Electrodes

Elizabeth V. Milsom[a], Jan Novak[a], Stephen J. Green[a], Xiaohang Zhang[a], Susan J. Stott[b], Roger J. Mortimer[b], Karen Edler[a], and Frank Marken[a]*

[a] *Department of Chemistry, University of Bath, Bath BA2 7AY, UK*

[b] *Department of Chemistry, Loughborough University, Loughborough LE11 3TU, UK*

To be submitted to Journal of Solid State Electrochemistry

Proofs to F. Marken

Email f.marken@bath.ac.uk

Abstract

The formation of variable thickness TiO_2 nanoparticle – Nafion® composite films with open pores is demonstrated via a layer-by-layer deposition process. Films of ca. 6 nm diameter TiO_2 nanoparticles grow in the presence of Nafion® by "clustering" of nanoparticles into bigger aggregates and the resulting hierarchical structure thickens with ca. 25 nm per deposition cycle. Film growth is characterized by electron microscopy, AFM, and quartz crystal microbalance techniques. SAXS/WAXS measurements for films before and after calcination demonstrate the effect of Nafion® binder causing aggregation. Electrochemical methods are employed to characterize the electrical conductivity and diffusivity of charge through the TiO_2-Nafion® composite films. Characteristic electrochemical responses are observed for cationic redox systems (diheptylviologen$^{2+/+}$, $Ru(NH_3)_6^{3+/2+}$, and ferrocenylmethyl-trimethylammonium$^{2+/+}$) immobilized into the TiO_2–Nafion® nanocomposite material. Charge conduction is dependent on the type of redox system and is proposed to occur either via direct conduction through the TiO_2 backbone (at sufficiently negative potentials) or via redox center based diffusion / electron hopping (at more positive potentials).

Key Words: voltammetry, TiO_2, Nafion®, electron hopping, sensor, mesoporous film, photoelectrochemistry, electrode.

1. Introduction

Mesoporous oxides are commonly used in sensors [1], photovoltaic devices [2], and in catalyst support systems [3]. In particular titanium oxide has found many applications [4] and is commonly applied in the form of mesoporous calcined films [5]. New alternative strategies for the deposition of ordered TiO_2 films include nanotube growth [6] and sol-gel dip-coating [7], but the more commonly employed direct deposition of nanoparticulate material is usually sufficient for most thin film applications. Porous membranes of TiO_2 have been formed by doctor-blading [8], printing [9], and by layer-by-layer deposition [10] of an alternating sequence of a negatively charged binder and the positively charged nanoparticulate TiO_2.

The layer-by-layer deposition of mesoporous oxides is versatile, reproducible, and ideal for the formation of thin coatings on electrode surfaces [11]. The methodology initially developed by Decher [12] allows molecular binders [13], ionomeric binders [14], and other types of nanoparticles [15] to be incorporated into the growing film. In this study the effect of employing Nafion® ionomer as a binder for TiO_2 nanoparticles is explored (see Figure 1).

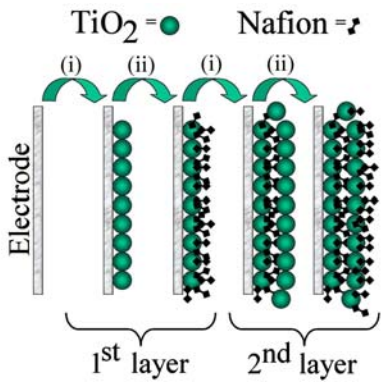

Figure 1. Schematic representation of the layer-by-layer deposition process involving, (i) immersion of the ITO substrate into the positively charged nanoparticle solution, followed by rinsing steps, and (ii) immersion into Nafion® anionomer solution followed by rinsing steps.

Although layer-by-layer deposition is possible with small molecular binders, higher molecular weight ionomers such as Nafion® are known to produce a more stable film [16]. The thickness of a single layer of a film depends on factors such as the weight, size and concentration of the polyelectrolyte binder and of the charged species. Intermolecular forces, hydrophobic forces [17], and hydrogen bonding [18] all have been reported to have an effect on the structure of the deposited films.

Composites of Nafion® (a chemically inert fluorocarbon with sulfonic acid groups [19]) and TiO_2 have been proposed for example for applications in proton-conducting membranes [20], in fuel cells [21], in photoelectrochemical devices [22], for photochemical degradation membranes [23], employed for dopamine sensing [24], and for nitric oxide sensing [25], and they have been produced with Langmuir-Schäfer techniques [26]. The combination of the chemically robust Nafion® binder with the mesoporous structure formed by the TiO_2 nanoparticle backbone results in a very interesting and widely applicable thin film structure.

In this study TiO_2 nanocomposite films are constructed from a Nafion® ionomer binder and ca. 6 nm diameter TiO_2 nanoparticles. A simple dip coating approach allows films of variable thickness to be formed and investigated. Perhaps surprisingly, an open-pore structure is formed consisting primarily of the TiO_2 backbone and a thin film of Nafion® at the surface. Voltammetric measurements in aqueous solution suggest that the charge transport at potentials negative of ca. -0.7 V vs. SCE is dominated by electron conduction through the TiO_2 backbone whereas at more positive potentials diffusion of redox species and inter-molecular electron hopping are dominating. The rate for charge transport in the positive potential range is very similar to that measured for conventional bulk Nafion® films.

2. Experimental

2.1. Chemical Reagents

Nafion® perfluorinated ion-exchange resin (5 wt%, in a mixture of lower aliphatic alcohols and H_2O), $NaClO_4$, KCl, 1,1'-diheptyl-4,4'-bipyridinium dibromide or diheptylviologen, $Ru(NH_3)_6Cl_3$, ferrocenylmethyl-trimethylammonium iodide (all Aldrich) were obtained commercially and used without further purification. TiO_2 sol (ca. 6 nm diameter, anatase, 30-35% in aqueous HNO_3, pH 0.5, TKS-202) was obtained from Tayca Corp, Japan. Solutions were prepared using filtered and deionized water with a resistivity of not less than 18 MΩ cm.

2.2. Instrumentation

Voltammetric experiments were performed with an microAutolab III system (Eco Chemie, Netherlands) in a standard three terminal electrochemical cell with a saturated calomel reference electrode, SCE, (Radiometer, Copenhagen) placed ca. 0.5 cm from the working electrode and a 2 cm × 2 cm platinum gauze counter electrode. The working electrodes were made from tin-doped indium oxide (ITO) coated glass (10 mm × 60 mm, 15 Ω per square, Image Optics, Basildon, UK). The ITO electrode was rinsed with ethanol and water, heat treated in a furnace (Elite Thermal Systems Ltd.) for 1 h at 500 ^{o}C, and re-equilibrated to ambient conditions before use. Prior to voltammetric experiments solutions were de-aerated with argon (BOC). All experiments were conducted at a temperature of 22 +/- 2 ^{o}C.

Quartz crystal microbalance experiments were conducted with ITO-coated quartz crystals (Part no. QA-A-9M-ITOM, Advanced Measurement Technology, Wokingham, Berks). A quartz crystal oscillator circuit (Oxford Electrodes) connected to a frequency counter (Fluke, PM6680B) allowed the resonance frequency of the quartz crystal sensor to be monitored. The 9.1 MHz AT-cut quartz

crystal microbalance system was calculated [27] to have a sensitivity factor of $\frac{\Delta m}{\Delta f}$ = -1.05 ng Hz^{-1} in air based on the expression $\frac{\Delta m}{\Delta f} = -\frac{A \times \sqrt{\mu_Q \rho_Q}}{2 f_0^{\,2}}$ with the area A = 0.2 cm^2, the resonance frequency f_0 = 9.1 × 10^6 Hz, the density of quartz ρ_Q = 2.648 gcm^{-3}, and the shear modulus of quartz μ_Q = 2.947 × 10^{11} g $cm^{-1}s^2$.

Field emission gun scanning electron microscopy (FEGSEM) images were obtained on a Leo 1530VP Field Emission Gun SEM system. A SAXS/WAXS (simultaneous small-angle x-ray scattering and wide-angle x-ray scattering) pattern of the TiO_2-Nafion® films was obtained on a SAXSess system using a PW3830 X-ray generator and the x-ray image plates were observed using a Perkin Elmer Cyclone Storage Phosphor System. A TiO_2-Nafion® film (50 deposition cycles on a microscopy cover plate) was produced and the patterns recorded in transmission mode with Cu Kα radiation (λ = 1.5406 Å) at 40 kV and 50 mA with an exposure time of 20 minutes. A background pattern from a clean cover plate was subtracted and the data corrected for slit smearing before fitting.

2.3. Layer-by-Layer Deposition of TiO_2–Nafion® Films

The deposition procedure consisted of a sequence of liquid immersion steps with (i) a TiO_2 sol (6 nm diameter, 3 wt% in nitric acid, pH ca. 2) for 60 seconds followed by rinsing with distilled water and methanol, (ii) dipping into Nafion® anionomer solution (ca. 3 wt% in methanol) for ~10 seconds followed by rinsing with methanol and distilled water. This completed a single layer deposition for the simple TiO_2-Nafion® film and the cycle was repeated to add more layers.

3. Results and Discussion

3.1. Layer-by-layer Formation of TiO_2 – Nafion® Nanocomposite Film Electrodes

Nafion® is an anionic polymer which is widely used as ion-exchange membrane material [28] or as a protective semipermeable coating [29]. Solutions of Nafion® in aliphatic alcohols are employed for the formation of thin films and in this study a dilute solution of Nafion® in methanol (0.3 wt%) is employed to act as a binder to grow thin films of a novel open pore TiO_2–Nafion® composite membrane. An aqueous TiO_2 sol provides the source of positively charged TiO_2 nanoparticles of nominal 6 nm diameter which are deposited with the Nafion® binder in a layer-by-layer deposition approach [30]. Tin-doped indium oxide (ITO) coated glass slides were employed as substrate (see Experimental). Due to the positive surface charge of the TiO_2 sol particles, ITO coated glass slides immersed into the nanoparticle solution will readily adsorb a very thin nanoparticle coating. When this electrode is rinsed with water and methanol, and then immersed into a Nafion® solution, binding of the anionic polymer and a restructuring of the surface occur. "Clustering" of TiO_2 nanoparticles into aggregates is observed. The electrode is then rinsed and re-immersed into the TiO_2 sol to continue the deposition process. An FEGSEM image of a 2-layer TiO_2-Nafion® films is shown in Figure 2A. It can be seen that the contact with the Nafion® anionomer causes nanoparticles to "cluster" into aggregates of ca. 40 nm diameter.

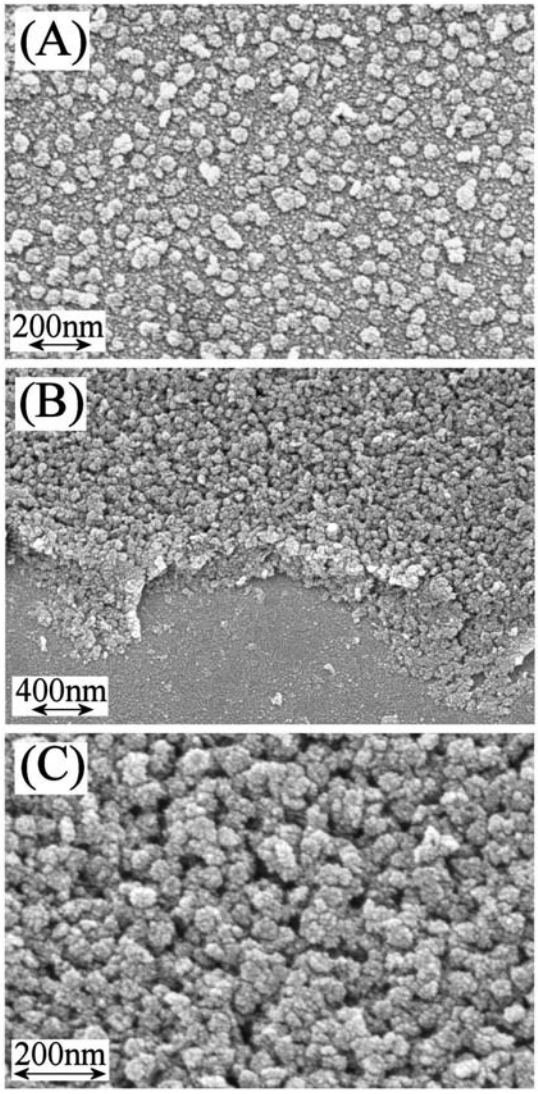

Figure 2: FEGSEM images of (A) a 2-layer TiO_2-Nafion® film and (B,C) a 15-layer TiO_2-Nafion® film (scratched with a scalpel) on ITO substrate.

When the deposition process is continued, more aggregates form and they assemble into a porous structure. Figure 2B and 2C show a 15-layer TiO_2-Nafion® film with pores of typically 10 to 30 nm diameter. These open pores create a hierarchical network and this can be beneficial by allowing gas and fluids to penetrate into the nanocomposite film. The thickness of the porous film is controlled by the number of deposition cycles employed. AFM images reveal the increase in thickness. An image of a 20-layer TiO_2-Nafion® film on an ITO substrate is shown in Figures 3A and 3B. The film was scratched to reveal the cross section. The 20-layer film showed a height of ca. 500 nm (see Figure 3C) which suggests a thickness of approximately 25 nm per deposition cycle which

compares well with earlier studies employing other types of binder molecules [31].

Quartz crystal microbalance measurements at an ITO-coated quartz crystal oscillator were employed to quantify the weight change during the deposition of consecutive layers of the TiO_2-Nafion® nanocomposite. A plot of the frequency of the ITO resonator against the number of layers deposited is shown in Figure 3D. This plot shows a linear build up of the TiO_2-Nafion® film with approximately 70 wt% contribution from TiO_2 and 30 wt% from Nafion®. These weight measurements were taken for dry films but may still contain small contribution from adsorbed water. The Sauerbrey equation allows the average weight to be calculated for TiO_2 particles deposited in one layer, 2600 ng cm^{-2} (corresponding to 6×10^{12} TiO_2 particles using the density of the TiO_2 anatase particles 3.9 g cm^{-3}) and for Nafion® deposited in one layer, 1000 ng cm^{-2}. These values are in good agreement with an average thickness per layer of 25 nm (vide supra).

Further characterisation of the TiO_2-Nafion® nanocomposite films was obtained using the simultaneous small-angle X-ray scattering and wide-angle X-ray scattering (SAXS/WAXS) technique. Figure 3E shows the intensity of the scattered X-ray diffraction pattern for both TiO_2-Nafion® and pure (calcined) TiO_2 nanoparticle films. The experimental data can be fitted to a model (see red line) to determine the structure of the nanoparticle films.

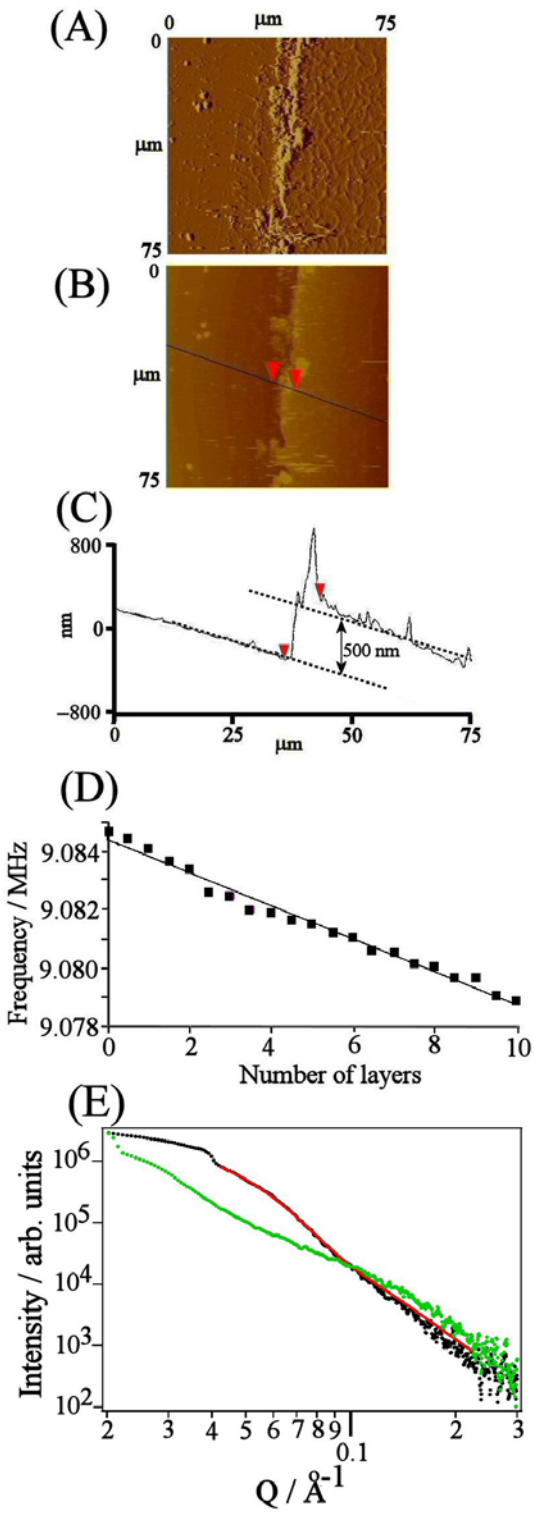

Figure 3. AFM image data showing a 20-layer deposit of TiO_2-Nafion® on an ITO surface: (A, B) topography, (C) cross section. The surface has been scratched prior to imaging. (D) Quartz crystal microbalance data obtained during deposition of consecutive TiO_2 and Nafion® layers onto an ITO coated quartz resonator. (E) SAXS/WAXS data: experimental data for TiO_2 film only (black), for a TiO_2-Nafion® film (green), and for a theoretical fit for polydisperse TiO_2 spheres (mean radius 38.81 Å, polydispersity 0.295) (red line).

The simulation model is that of isolated polydisperse spheres with a mean radius of 38.81 Å (assuming no interaction between each sphere) and is seen to give an excellent fit for the calcined TiO_2 film (treated at 500 ^oC in air for 30 minutes) between 0.04 and 0.1 $Å^{-1}$ indicating that there is no significant colloidal crystallinity. The small divergence between the fit and experimental data at greater values of Q may suggest possible interaction between spheres. A step in the intensity level is observed in the TiO_2-Nafion® and pure TiO_2 film at 0.04 $Å^{-1}$ and 0.08 $Å^{-1}$, respectively, that relates to the size of the particle or aggregate spheres. It is possible to establish that the TiO_2-Nafion® aggregates are in average almost double the size of pure TiO_2 nanoparticles. However, a more complex composite structure is present which is not easily modeled with conventional approaches. From FEGSEM image evidence (see Figure 2) a raspberry-type packing or hierarchical clustering seems to occur. The step in intensity level at 0.02 $Å^{-1}$ and 0.04 $Å^{-1}$ in the TiO_2-Nafion® and pure TiO_2 films, respectively, can be attributed to an artifact generated after the subtraction of the background scattering pattern.

3.2. Electrochemical Processes in TiO_2 – Nafion® Nanocomposite Film Electrodes

The voltammetric response observed for a clean ITO electrode immersed in aqueous 0.1 M KCl (used as an inert electrolyte) between +0.5 V vs. SCE and -1.0 V vs. SCE is featureless and consistent with a clean background (not shown). Figure 4 shows the voltammetric responses for a series of TiO_2-Nafion® films on ITO immersed in 0.1 M KCl. A reduction response commences at -0.7 V vs. SCE which is typical for a TiO_2 film and is explained by the filling of the conduction band within the oxide [32]. Upon reversal of the scan direction an oxidation peak is observed which is consistent with electrons moving back from the oxide to the ITO substrate. The basic shape of the voltammograms can be explained by capacitive charging of the oxide and a resistance, which is mainly due to the ITO film [33]. The three different electrodes were (i) 2, (ii) 10, and (iii) 20 layers of TiO_2-Nafion®. The increase of TiO_2 film thickness is demonstrated by the approximately

proportional increase in the voltammetric response, which is associated with the reduction of Ti(IV) (vide infra).

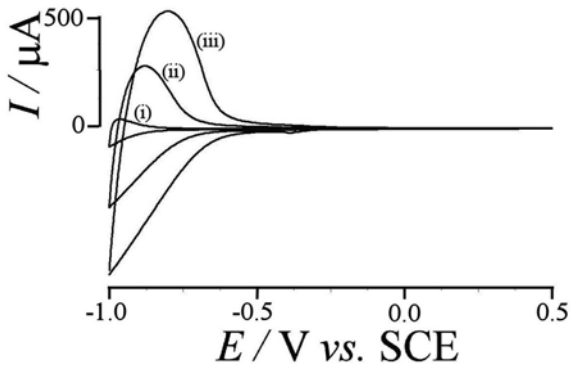

Figure 4. Cyclic voltammograms (scan rate 100 mVs^{-1}) for the reduction and oxidation of 6 nm TiO_2 nanoparticles bound by Nafion®, immobilized on ITO electrodes (area 1 cm^2) immersed in 0.1 M KCl. (i) 2 layers TiO_2, (ii) 10 layers TiO_2, (iii) 20 layers TiO_2.

In order to explore the reactivity of the TiO_2-Nafion® film in the presence of redox systems, three cationic redox systems with reversible one-electron characteristics have been chosen with reversible potentials close and more positive away from the TiO_2 conduction band edge.

The 1,1'-diheptyl-4,4'-bipyridinium (or diheptylviologen) system exhibits a reversible redox process at -0.62 V vs. SCE (see Figure 5A) and a second reversible reduction step at more negative potentials (not shown) [34]. In order to obtain this response, a 5-layer TiO_2-Nafion® film was immersed into a solution of 1,1'-diheptyl-4,4'-bipyridinium dibromide (1 mM in ethanol) for one minute. The 1,1'-diheptyl-4,4'-bipyridinium was quickly immobilised into the Nafion® binder in the TiO_2-Nafion® film. The resulting electrode was then placed into aqueous 0.1 M KCl electrolyte and a cyclic voltammogram was recorded.

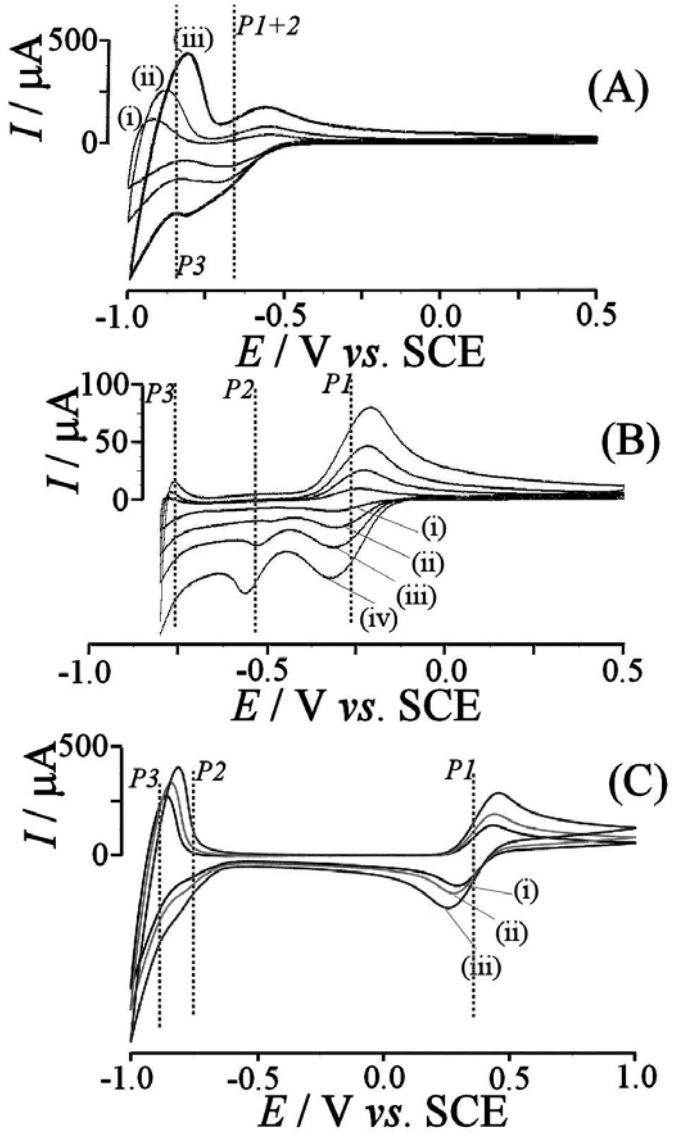

Figure 5. (A) Cyclic voltammograms (scan rates (i) 20, (ii) 50, (iii) 100 mVs^{-1}) for the reduction and oxidation of 1,1'-diheptyl-4,4'-bipyridinium in a 5-layer TiO_2-Nafion® film immobilized onto an ITO surface (area 1 cm^2). The electrode was first immersed into a 1 mM solution of 1,1'-diheptyl-4,4'-bipyridinium dibromide in ethanol for 1 minute, then rinsed with ethanol, and then the electrode was immersed in a 0.1 M KCl electrolyte. (B) Cyclic voltammograms (scan rates (i) 20, (ii) 50, (iii) 100, and (iv) 200 mVs^{-1}) for the reduction and oxidation of $Ru(NH_3)_6^{3+}$ in a 20-layer TiO_2-Nafion® film. The electrode was first immersed into 1 mM $Ru(NH_3)_6^{3+}$ in water, then rinsed with water, and then the electrode was immersed into a 0.1 M KCl electrolyte. (C) Cyclic voltammograms (scan rates (i) 20, (ii) 50, and (iii) 100 mVs^{-1}) for the reduction and oxidation of ferrocenylmethyl-trimethylammonium$^+$ in a 20-layer TiO_2-Nafion® film. The electrode was first immersed into 1 mM ferrocenylmethyl-trimethylammonium iodide in water, then rinsed with water, and then the electrode was immersed into a 0.1 M KCl electrolyte. Dashed lines indicate the approximate potential for redox processes.

In Figure 5A, Process 1 (P1) denotes the reduction of 1,1'-diheptyl-4,4'-bipyridinium^{2+} to 1,1'-diheptyl-4,4'-bipyridinium^{+} by electrons directly from the ITO electrode surface (see equation 1). This particular mechanism operates solely at the ITO surface and requires molecular or charge diffusion within the Nafion® film. A second type of electron transfer is possible at more negative potentials, denoted Process 2 (see equation 2). TiO_2 at sufficiently negative potentials is conducting electrons and therefore direct electron transfer from TiO_2 becomes possible [35].

Process 1: $[Ox]^{n+}(\text{Nafion®}) + e^{-}(\text{ITO electrode}) \rightleftharpoons [Red]^{(n-1)+}(\text{Nafion®})$ (1)

Process 2: $[Ox]^{n+}(\text{Nafion®}) + e^{-}(TiO_2) \longrightarrow [Red]^{(n-1)+}(\text{Nafion®})$ (2)

Process 3: $Ti(IV)(TiO_2) + e^{-}(\text{ITO electrode}) + H_2O \rightleftharpoons Ti(III)(TiO_2) + H^{+}(TiO_2) + OH^{-}$ (3)

A third process observed at potentials negative of -0.7 V vs. SCE can be attributed to the conduction band filling of TiO_2 (see Figure 4) which is associated with proton uptake (see equation 3). Next, a 20-layer TiO_2-Nafion® film is immersed into a solution of $Ru(NH_3)_6^{3+}$ (1 mM in water) for one minute. The cationic $Ru(NH_3)_6^{3+}$ is immobilised into the Nafion® binder and after rinsing with water a reversible voltammetric response is observed at -0.25 V vs. SCE (see Figure 5B). This voltammetric signal occurs positive of the potential zone where TiO_2 is conducting and therefore can be attributed purely to Process 1 (equation 1). A new a separate irreversible reduction peak at -0.5 V vs. SCE corresponds to Process 2, the $Ru(NH_3)_6^{3+}$ reduction via TiO_2 (equation 2).

Finally, a redox system with even more positive reversible potential was selected. Ferrocenylmethyl-trimethylammonium^{+} ($TMAFc^{+}$) is readily adsorbed into Nafion® and shows highly reversible electron transfer characteristics. A 20-layer TiO_2-Nafion® film was immersed into

a solution of $TMAFc^+$ iodide (1 mM in water) for one minute. The $TMAFc^+$ cation was immobilised into the Nafion® anionomer binder. The resulting electrode was then immersed into aqueous 0.1 M KCl electrolyte and voltammograms recorded (see Figure 5C). A reversible response at 0.37 V vs. SCE corresponds to Process 1 (equation 1), the one electron oxidation/reduction of $TMAFc^+$ by electrons directly from the ITO surface. A second reduction response is observed at -0.75 V vs. SCE (see Process 2). The signal is irreversible and observed only immediately after scanning into the $TMAFc^+$ oxidation. It is interesting to note that the potential for Process 2 is dependent on the type of redox system and this may reflect (i) the rate of electron transfer from TiO_2 to the molecular redox system and (ii) the ability of the redox system to interact with the TiO_2 nanoparticle surface. More hydrophobic redox systems such as $TMAFc^+$ appear to interact less effectively with TiO_2 which may be responsible for the shift of Process 2 to more negative potentials.

Next, electron and charge transport within the mesoporous TiO_2-Nafion® film is investigated in more detail. By changing the film thickness and the potential scan rate quantitative insights into the charge transfer and diffusion within the nanocomposite films can be obtained.

3.3. Charge Diffusion in TiO_2 – Nafion® Nanocomposite Film Electrodes

By focusing on one particular redox system, ferrocenylmethyl-trimethylammonium$^+$, it is possible to further explore the effects of charge diffusion in the TiO_2-Nafion® composite material. Initially, a study of the adsorption characteristics of the ferrocenylmethyl-trimethylammonium cation ($TMAFc^+$) into the TiO_2-Nafion® films was undertaken. Figure 6 shows the experimental results indicating a reversible voltammetric response at a potential of 0.35 V vs. SCE with increasing peak area as a function of $TMAFc^+$ immobilization concentration. Essentially Langmurian characteristics are observed and for ferrocenylmethyl-trimethylammonium$^+$ a binding constant of 9000 $dm^3\ mol^{-1}$

can be extracted.

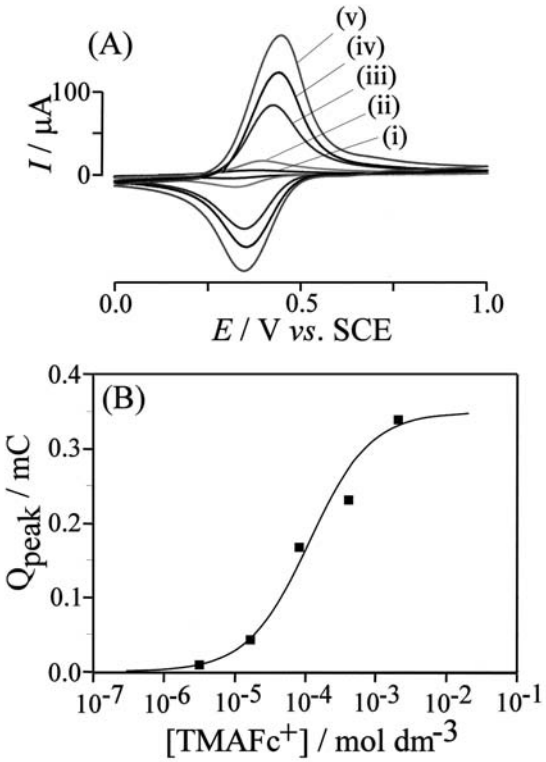

Figure 6. (A) Cyclic voltammograms (scan rate 0.1 V s^{-1}) for the oxidation and re-reduction of ferrocenylmethyl-trimethylammonium$^+$ immobilized into a 5-layer TiO_2-Nafion® film at an ITO electrode surface (area 1 cm^2) and immersed into aqueous 0.1 M $NaClO_4$. The ferrocenylmethyl-trimethylammonium$^+$ concentration during the immobilizations step was (i) 3.2 μM, (ii) 16 μM, (iii) 80 μM, (iv) 0.4 mM, and (v) 2 mM in water. (B) Plot of the ferrocenylmethyl-trimethylammonium$^+$ concentration in the immobilization solution versus the charge under the voltammetric signal. The line shows a Langmuir dependence with a binding constant of K = 9000 dm^3 mol^{-1}.

The transport of charges in the porous TiO_2-Nafion® membrane is an interesting feature and must be connected to both (i) the mobility of an immobilized redox system such as ferrocenylmethyl-trimethylammonium$^+$ ($TMAFc^+$) and (ii) intermolecular electron hopping. In the positive potential range TiO_2 is clearly electrically insulating and charge transport along the pore walls within the mesoporous composite must be occurring. This was further confirmed by calcination of the TiO_2-Nafion® nanocomposite (this treatment at 500 ^oC in air fully removed all organic components and

leaves a purely inorganic anatase film, see Figure 3E) followed by re-adsorption of Nafion® from the dip coating solution (this process took approximately 24h for a 20-layer film due to slow penetration of the anionomer back into the porous TiO_2). The resulting calcined film is believed to have much better TiO_2 particle-particle contacts but otherwise very similar dimensions. However, the voltammetric features did not change significantly (see below) and therefore a contribution from the TiO_2 backbone to charge conductivity is highly unlikely.

In order to study the effect of the film thickness on the voltammetric features a sequence of experiments was undertaken using a 2 mM ferrocenylmethyl-trimethylammonium$^+$ deposition solution and a 0.1 M $NaClO_4$ electrolyte solution (see Figure 7). The increase in film thickness clearly resulted in an increase of the voltammetric peak current.

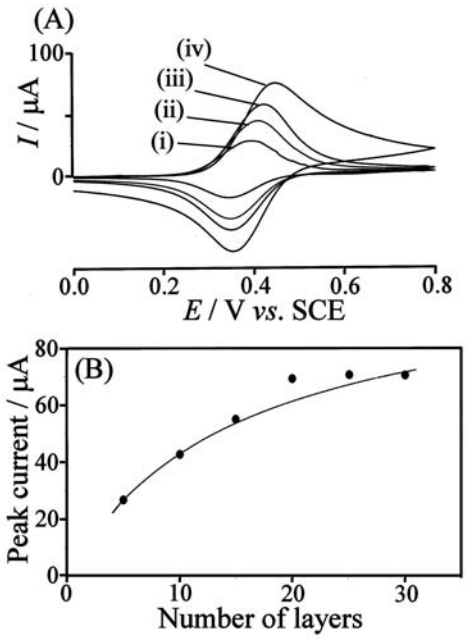

Figure 7. (A) Cyclic voltammograms (scan rate 0.02 V s^{-1}) for the oxidation and re-reduction of ferrocenylmethyl-trimethylammonium$^+$ immobilized into a (i) 5, (ii) 10, (iii) 15, and (iv) 30-layer TiO_2-Nafion® film at an ITO electrode surface (area 1 cm^2) and immersed into aqueous 0.1 M $NaClO_4$. The ferrocenylmethyl-trimethylammonium$^+$ concentration during the immobilizations step was 2 mM in water. (B) Plot of the peak current versus the number of deposition layers. The line corresponds to a fit employing equation 6 with a concentration of c = 0.1 M and an apparent diffusion coefficient of $D = 3.5 \times 10^{-14}$ m^2s^{-1}.

The relation ship of the peak current with film thickness (see Figure 7B) is not proportional and at sufficiently thick films (ca. 1 μm) a stable peak current remains, completely independent of thickness. This transition in behaviour is consistent with a diffusion layer thickness in the mesoporous film. Approximate expressions can be written to describe this effect. The peak current for a complete electrolysis of the thin film at the electrode surface is given by equation 4 [36].

$$I_{p,\text{thin film}} = \frac{n^2F^2}{4RT} vVc = \frac{n^2F^2}{4RT} vA\delta c \tag{4}$$

In this equation, the peak current is related to the number of transferred electrons per molecule diffusing to the electrode surface, n, the Faraday constant, F, the gas constant, R, the absolute temperature, T, the scan rate, v, the electrode area, A, the film thickness, δ, and the concentration of redox active material, c. In contrast, for a thick film a diffusion-controlled peak current (assuming a homogeneous material) is expected (see equation 5 [37]).

$$I_{p,\text{diffusion}} = 0.446nFAc\sqrt{\frac{nFvD}{RT}} \tag{5}$$

In this equation the apparent diffusion coefficient is denoted by D. The transition of behaviour as a function of film thickness may be approximated by combining these two expressions in equation 6.

$$I_p = \frac{I_{p,\text{thin film}} \times I_{p,\text{diffusion}}}{I_{p,\text{diffusion}} + I_{p,\text{thin film}}} = \frac{n^2F^2vDAc\,\delta}{4RTD + 2.242\sqrt{RTDFnv}\,\delta} \tag{6}$$

Analysis of the thickness dependent voltammetric peak current data (see Figure 7B and equation 6)

suggests an approximate apparent diffusion coefficient of $D = 3.5 \times 10^{-14}$ m^2s^{-1} for ferrocenylmethyl-trimethylammonium$^+$. This value is very similar to the apparent diffusion coefficients reported for example for $Ru(bipy)_3^{3+/2+}$ in pure Nafion® [38,39].

Next, the scan rate is systematically varied. In Figure 8 voltammetric data for the oxidation of ferrocenylmethyl-trimethylammonium$^+$ immobilised in a 5-layer TiO_2-Nafion® film are shown. A plot of the logarithm of the peak current versus the logarithm of the scan rate is expected to result in two linear regions: (i) a linear region with slope 1 due to thin film behaviour (see equation 4) and (ii) a region with slope ½ due to diffusion within the film (see equation 5).

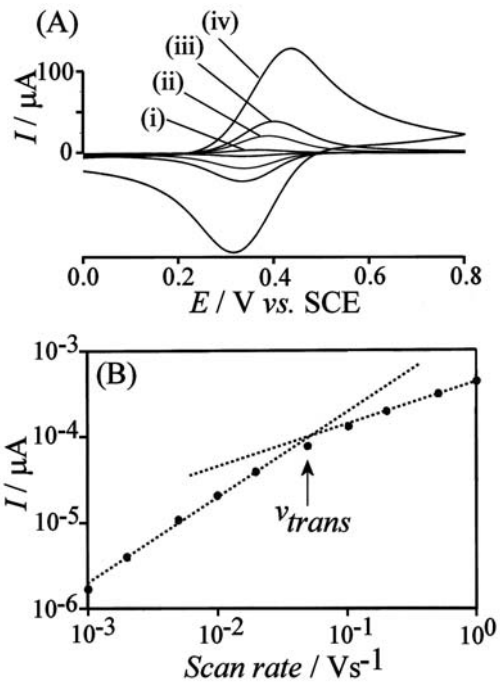

Figure 8. (A) Cyclic voltammograms (scan rate (i) 0.002, (ii) 0.01, (iii) 0.02, (iv) 0.1 V s^{-1}) for the oxidation and re-reduction of ferrocenylmethyl-trimethylammonium$^+$ immobilized into a 5-layer TiO_2-Nafion® film at an ITO electrode surface (area 1 cm^2) and immersed into aqueous 0.1 $NaClO_4$. The ferrocenylmethyl-trimethylammonium$^+$ concentration during the immobilizations step was 2 mM in water. (B) Plot of the peak current for the oxidation peak versus scan rate.

The plot in Figure 8B clearly shows a transition between thin film and diffusion characteristics at a transition scan rate of $v_{trans} \approx 0.05$ Vs^{-1}. By combining equations 4 and 5 an approximate expression

for this transition can be obtained (equation 7).

$$D = \frac{n\nu_{trans}F}{RT}\left(\frac{\delta}{1.784}\right)^2 \quad (7)$$

For data in Figure 8B the apparent diffusion coefficient is calculated as $D \approx 1 \times 10^{-14}$ m^2s^{-1} in good agreement with the estimate obtained above. The thickness of the film δ introduces a considerable error into this calculation and therefore the methodology based on thickness variation is probably more accurate.

4. Conclusions

It has been shown that well defined open-pore mesoporous structures are obtained by a layer-by-layer deposition of TiO_2 with Nafion® ionomer binder. TiO_2 particles of nominal 6 nm diameter tend to cluster into aggregates of ca. 20-40 nm size. The properties of the resulting films have been investigated and redox reactions for three cationic redox systems studied. At potentials sufficiently positive of the conduction band edge, charge propagation/diffusion within the films is entirely due to electron hopping and molecular diffusion and very similar in magnitude when compared to processes in conventional Nafion® membrane systems. The open structure of these films allows fast diffusional access into the porous structure and in future this kind of membrane could be beneficial as a sensor films or it could be employed as a host for proteins or enzymes.

5. Acknowledgements

Tayca Corporation is acknowledged for providing a sample of TiO_2 colloidal solution. E.V.M. and S.J.S. are grateful for studentships awarded by the EPSRC and Royal Society of Chemistry. We

acknowledge PANalytical for the generous provision of a SAXSess system used in the SAXS measurements included in this paper.

References

1 Varghese OK, Grimes CA (2003) J Nanosci Nanotech 3: 277

2 Grätzel M (2005) MRS Bull 30: 23

3 Schuth F (2005) Ann Rev Mater Res 35: 209

4 Diebold U (2003) Surf Sci Rep 48: 53

5 Bisquert J, Cahen D, Hodes G, Ruhle S, Zaban A (2004) J Phys Chem B 108: 8106

6 Bavykin DV, Milsom EV, Marken F, Kim DH, Marsh DH, Riley DJ, Walsh FC, El-Abiary KH, Lapkin AA (2005) Electrochem Commun 7: 1050

7 Bockmeyer M, Lobmann P (2006) Chem Mater 18: 4478

8 Cameron PJ, Peter LM, Hore S (2005) J Phys Chem B 109: 930

9 Ma TL, Kida T, Akiyama M, Inoue K, Tsunematsu SJ, Yao K, Noma H, Abe E (2003) Electrochem Commun 5: 369

10 McKenzie KJ, King PM, Marken F, Gardner CE, Macpherson JV (2005) J Electroanal Chem 579: 267

11 Stott SJ, Mortimer RJ, McKenzie KJ, Marken F (2005) Analyst 130: 358

12 Decher G, Schlenoff (2003) Multilayer thin films, Wiley-VCH, Weinheim

13 McKenzie KJ, Marken F, Hyde M, Compton RG (2002) New J Chem 26: 625

14 Murphy MA, Wilcox GD, Dahm RH, Marken F (2005) Ind J Chem A 44: 924

15 Milsom EV, Novak J, Oyama M, Marken F (2006) Electrochem Commun in print

16 Correa-Duarte MA, Gierig M, Kotov NA, Liz-Marzan LM (1998) Langmuir 14: 6430

17 Neivandt DJ, Gee M, Tripp CP, Hair ML (1997) Langmuir 13: 2519

18 Serizawa T, Yamamoto K, Akashi M (1999) Langmuir 15: 4682

19 Davis TA, Genders JD, Pletcher D (1997) Ion permeable membranes, The Electrochemical Consultancy, Romsey, UK

20 Shao ZG, Xu H, Li M, Hsing IM (2006) Solid State Ionics 177: 779

21 Chalkova E, Fedkin MV, Wesolowski DJ, Lvov SN (2005) J Electrochem Soc 152: A1742

22 Park H, Choi W (2006) Langmuir 22: 2906

23 Park H, Choi W (2005) J Phys Chem B 109: 11667

24 Yuan S, Hu S (2004) Electrochim Acta 49: 4287

25 Wang Y, Li C, Hu S (2006) J Solid State Electrochem 10: 383

26 Bertoncello P, Notargiacomo A, Nicolini C (2005) Langmuir 21: 172

27 Ward MD, in Rubinstein I (ed) (1995) Physical Electrochemistry, Marcel Dekker, New York, p 297

28 Buttry DA, Anson FC (1982) J Am Chem Soc 104: 4824.

29 Mortimer RJ (1995) J Electroanal Chem 397: 79

30 Farhat TR, Hammond PT (2006) Adv Func Mater 16: 433

31 McKenzie KJ, Marken F (2003) Langmuir 19: 4327

32 Marken F, Bhambra AS, Kim DH, Mortimer RJ, Stott SJ (2004) Electrochem Commun 6: 1153

33 Fabregat-Santiago F, Mora-Sero I, Garcia-Belmonte G, Bisquert J (2003) J Phys Chem B 107: 758

34 Mortimer RJ, Dillingham JL, J Electroanal Chem (1997) 144: 1549

35 Milson E, Perrott HR, Peter LM, Marken F (2005) Langmuir 21:9482

36 Bard AJ, Faulkner LR (2001) Electrochemical methods, 2nd edition, Wiley, New York, p 591

37 Scholz F (2002) Electroanalytical methods, Springer, Berlin, p 64

38 Majda M in Murray R (1992) Molecular design of electrode surfaces, Wiley, New York, p 200

39 Buttry DA, Anson FC (1983) J Am Chem Soc 105: 685